



Taurine stimulates protein synthesis and proliferation of C2C12 myoblast cells through the PI3K-ARID4B-mTOR pathway

Qi Hao^{1,2†}, Lulu Wang^{1,2†}, Minghui Zhang¹, Zhe Wang², Meng Li² and Xuejun Gao^{1,2*}

¹College of Animal Science, Yangtze University, Jingzhou 434025, People's Republic of China

²College of Life Science, Northeast Agricultural University, Harbin 150030, People's Republic of China

(Submitted 23 June 2021 – Final revision received 31 October 2021 – Accepted 23 November 2021 – First published online 9 December 2021)

Abstract

Taurine (Tau) has many profound physiological functions, but its role and molecular mechanism in muscle cells are still not fully understood. In this study, we investigated the role and underlying molecular mechanism of Tau on protein synthesis and proliferation of C2C12 myoblast cells. Cells were treated with Tau (0, 60, 120, 180 and 240 μ M) for 24 h. Tau dose-dependently promoted protein synthesis, cell proliferation, mechanistic target of rapamycin protein (mTOR) phosphorylation and also AT-rich interaction domain 4B (ARID4B) expression, with the best stimulatory effects at 120 μ M. LY 294002 treatment showed that Tau promoted ARID4B expression in a phosphoinositide 3-kinase (PI3K)-dependent manner. ARID4B knockdown (by small interfering RNA transfection for 24 h) prevented Tau from stimulating protein synthesis and cell proliferation, whereas ARID4B gene activation (using the CRISPR/dCas9 technology) had stimulatory effects. ARID4B knockdown abolished Tau signalling to mRNA expression and protein phosphorylation of mTOR, whereas ARID4B gene activation had stimulatory effects. Chromatin immunoprecipitation (ChIP)-PCR identified that all of ARID4B, H3K27ac and H3K27me3 bound to the –4368 to –4591 bp site in the *mTOR* promoter, and ChIP-quantitative PCR (qPCR) further detected that Tau stimulated ARID4B binding to this site. ARID4B knockdown or gene activation did not affect H3K27me3 binding to the *mTOR* promoter but decreased or increased H3K27ac binding, respectively. Furthermore, ARID4B knockdown abolished the stimulation of Tau on H3K27ac binding to the *mTOR* promoter. In summary, these data uncover that Tau promotes protein synthesis and proliferation of C2C12 myoblast cells through the PI3K-ARID4B-mTOR pathway, providing a deep understanding of how Tau regulates anabolism in muscle cells.

Key words: ARID4B: H3K27ac: mTOR: Myoblast cell: PI3K: Taurine

In the course of skeletal muscle growth and development, stem cells differentiate into mononuclear myoblasts, and afterwards myoblasts fuse to form multinucleated myotubes and mature muscle fibres. The growth and development process of skeletal muscle cells include proliferation and differentiation of myoblasts as well as protein synthesis⁽¹⁾. The serine/threonine protein kinase mechanistic target of rapamycin protein (mTOR) is a core regulatory factor and the most key signalling molecule involved in the regulation of cell growth and protein synthesis⁽²⁾. Environmental cues such as nutrients and hormones can stimulate mTOR phosphorylation (activation)^(3,4), and p-mTOR phosphorylates its downstream targets such as the ribosomal protein S6 kinase 1 (S6K1) to stimulate protein translation and cell growth^(5,6). Studies have found that activation of the mTOR-S6K1 signalling pathway can promote skeletal muscle growth and regeneration^(7,8).

Taurine (Tau, 2-aminoethanesulfonic acid) is an abundant β -sulfamic acid in many mammalian tissues, found in very high concentration in muscle cells⁽⁹⁾. Tau has many profound physiological functions, including bile secretion, antioxidant activity, Ca homeostasis, antiapoptotic effects, protection against neurodegenerative diseases or atherosclerosis, etc^(10–13). Cells can accumulate Tau through the Na⁺-dependent Tau transporter (TauT)⁽¹⁴⁾. Tau can regulate the PI3K/AKT, AKT/FOXO1, JAK2/STAT3 and mTOR/AMPK signal pathways for cell proliferation and protein synthesis^(15,16), though there is still a discrepancy in the results of the effects of Tau on the mTOR pathway^(17–20).

Supplementation of Tau in the diet can improve energy metabolism and antioxidant capacity in the skeletal muscle, liver, heart and adipose tissue⁽²¹⁾. In animal feeding, Tau can be used as a feed additive for non-ruminants, including poultry, dog, cat

Abbreviations: ARID, AT-rich interaction domain; ChIP, chromatin immunoprecipitation; mTOR, mechanistic target of rapamycin protein; PI3K, phosphoinositide 3-kinase; siRNA, small interfering RNA; S6K1, S6 kinase 1; Tau, Taurine; TauT, Tau transporter.

* **Corresponding author:** Xuejun Gao, email gaoxj53901@163.com

† These authors contributed equally to this work.

and aquatic animals. Tau addition at the level of 5.00 g/kg of the diet for 42 d increased body weight gain and gain:feed ratio in broiler chickens⁽²²⁾. Since Tau is only found in animal products, Tau needs to be supplemented in commercial vegan foods of cats and dogs which have limited hepatic production of Tau⁽²³⁾. Crabs fed diets supplemented with 0.4–0.8% (w/w) Tau for 65 d had improved growth performance⁽²⁴⁾. There are rare reports on the application of Tau as a feed additive to ruminants, and thus it is still largely unclear the effects of Tau supply on their performance. A previous report showed that supplementation of rumen-protected methionine at the level of 0.08% DM of the diet during the periparturient period increased plasma Tau concentration (control group, 31.6 mg/dl; methionine group, 47.4 mg/dl) in dairy cows⁽²⁵⁾. Since there are few animal-derived ingredients in the feed of ruminants, sulphur amino acids including methionine might be the sources of Tau for ruminants to meet the needs of the body.

Previous reports have shown that Tau has significant effects on muscle cells. Tau can prevent muscle senescence and skeletal muscle disorders through regulating cellular redox homeostasis⁽²⁶⁾. Tau can enhance the differentiation of myoblast cells to myotubes through TauT and Ca²⁺ signalling pathway⁽²⁷⁾. Tau can attenuate skeletal muscle injury induced by diquat toxicity⁽²⁸⁾. Recent reports have found that Tau can promote proliferation and protein synthesis of muscle cells through attenuating catabolic processes^(29,30). These above reports point out that Tau is a key regulator of protein synthesis and proliferation of muscle cells. Nevertheless, the dose-dependent effects of Tau on these processes and underlying molecular mechanism still need further study.

AT-rich interaction domain family (ARID family) is a type of transcription factor that binds to DNA rich in AT sequence and has a variety of regulatory effects. ARID family can be divided into seven subfamilies, namely ARID1, ARID2, ARID3, ARID4, ARID5, JARID1 and JARID2⁽³¹⁾. ARID family is related to the regulation of chromatin remodelling and gene expression during cell growth, differentiation and development⁽³²⁾. The ARID4 subfamily has two members: ARID4A and ARID4B, also called retinoblastoma binding protein 1 (RBP1) and RBP1-like protein 1, respectively⁽³¹⁾. Studies have shown that ARID4B is a component of the SIN3A/histone deacetylase 1 (HDAC1) chromatin remodelling complex, and participates in the regulation of histone deacetylation and epigenetic regulation of cell physiology^(33–36). Several recent studies have discovered that ARID4B plays a key role in cell growth and differentiation^(36–38), while the detailed molecular mechanism still needs to be deeply elucidated. It is still unknown whether Tau can function through epigenetic regulation mediated by some chromatin remodellers such as ARID4B.

We previously found from our proteomics data that ARID4B might be associated with the growth of C2C12 myoblast cells. In this study, we aim to investigate the dose-dependent effects of Tau on protein synthesis and proliferation of C2C12 myoblast cells and uncover the ARID4B-associated epigenetic regulatory mechanism in Tau signalling to these phenotypes. Our findings would lay a deep theoretical foundation for the utilisation of Tau in muscle production in animal feeding.

Methods

Materials

Tau (purity > 99%) was purchased from a company (T6017, Macklin), dissolved in OPTI-MEM I (Gibco) medium (100 mM, stock solution) and stored at –20°C for further use. Mouse myoblast cell line C2C12 was donated by the laboratory of Professor Yunqin Yan, College of Life Science, Northeast Agricultural University.

Cell culture and treatments

C2C12 myoblast cells were cultured in growth medium containing DMEM/F12 (Gibco) and 10% fetal bovine serum (Gibco), 0.1 mg/ml streptomycin and 100 IU/ml penicillin at 37°C in a controlled humidified 5% CO₂ atmosphere. For experimental assays, cells were starved with OPTI-MEM I (Gibco) for 24 h before treatments. To examine the dose-dependent effects of Tau, C2C12 myoblast cells reached 60–70% confluence were treated with Tau (0, 60, 120, 180 and 240 μM) for 24 h. These concentrations were selected by multiple rounds of screening based on our previous report⁽¹⁵⁾. Morphological images of C2C12 myoblast cells were observed by an inverted microscope (AE31E, Motic). A specific inhibitor of the phosphoinositide 3-kinase (PI3K), LY 294002 (15 μM) (S1737, Beyotime), was used to inhibit PI3K activation⁽¹⁵⁾. The product package of LY 294002 was 30 mM × 0.1 ml, dissolved in dimethylsulfoxide and stored at –20°C. Before use, the solution was diluted in OPTI-MEM I (Gibco) medium (1.5 mM, application solution).

Measurement of protein synthesis rate

SUNSET (surface sensing of translation) is a non-radioactive technique for *in vivo* measurement of protein synthesis rate in cells^(39,40). This technique involves using the antibiotic puromycin (a structural analogue of tyrosyl-tRNA) (ST551, Beyotime) and an anti-puromycin antibody (MABE343, Millipore) to detect the amount of puromycin incorporated into the nascent peptide chains. After treatments, 1.5 μM puromycin was added into the culture medium and incubated for 30 min, then puromycin incorporated into peptide chains was detected by Western blotting analysis. Three independent experiments were performed.

Western blotting

Protein samples (20 μg protein/lane) were separated in 8–10% SDS polyacrylamide gels at 120 V for 1.5–2 h. Then proteins were transferred onto a nitrocellulose membrane. The membrane was blocked in 5% skim milk (5% skim milk and 0.1% Tween-20 in TBS), then incubated with a specific primary antibody at 4°C overnight. Primary antibodies used were ARID4B (24499-AP, Proteintech), p-mTOR (Ser-2448) (bs-3494R, Bioss), mTOR (bs-1992R, Bioss), AKT (bs-0115R, Bioss), p-AKT (bs-2720R, Bioss), p70 S6K1(14485–1-AP, Proteintech), p70 p-S6K1 (Thr-389) (#9206, CST), H3K27ac (39034, Active Motif), H3K27me3 (39055, Active Motif), H3 (17168-1-AP, Proteintech) and β-actin (bs-0061R, Bioss). Then the membrane was washed with TBST and next incubated with the secondary antibody bound to



horseradish peroxidase at 37°C for 1 h. Protein bands were visualised with enhanced chemiluminescence, and ImageJ software was used for quantitative analysis. Three independent experiments were performed.

Protein content detection

Total protein content was detected using the Enhanced BCA Protein Assay Kit (P0010S, Beyotime), according to the manufacturer's protocol. The absorbance of each well at 562 nm was measured using a microplate meter (SpectraMax iD3, Molecular Devices). Results were compared with the protein standard curve. Five independent experiments were performed.

Cell number counting

The number of C2C12 cells was counted by using the Cell Counting Kit-8 (C0037, Beyotime), following the manufacturer's instructions. In brief, C2C12 cells were inoculated into a 96-well plate at a density of 4×10^3 cells/well. After treatments, 10- μ l Cell Counting Kit-8 solution and 100- μ l OPTI-MEM I medium were added to each well and then the cultures were incubated at 37°C for 1 h. The OD value of each well at 450 nm was measured with a microplate reader. Five independent experiments were performed.

qRT-PCR

qRT-PCR assays were performed by using the BeyoFast SYBR Green One-Step qRT-PCR Kit (D7268S, Beyotime). Each 20 μ l reaction mixture contained 10 μ l of reaction buffer (2 \times), 1 μ l each of 5 μ M forward and reverse primers, 6 μ l of nuclease-free water, and 2 μ l of DNA or RNA. RNA was extracted with the RNAeasy Animal RNA Isolation Kit with Spin Column (R0026, Beyotime), according to the manufacturer's instructions. The CFX96 Touch RT-PCR System (Bio-Rad) was used for amplification on a 96-well plate. The qRT-PCR amplification conditions were as follows: 95°C for 2 min; 95°C for 15 s, 60°C 30 s, 40 cycles and 72°C for 30 s. Relative gene expression was calculated as the $2^{-\Delta\Delta CT}$ fold change. The primer sequences were *mTOR*, F: 5'-CTGATCCTCAACGAGCTAGTTC-3', R: 5'-GGTCTTTGCAG TACTTGTTCATG-3'; *ARID4B*, F: 5'-GAAGATAACAGCAGC GAAGAAG-3', R: 5'-AGGCCGTTTGTAAATAGGTGTA-3'; β -*actin*, F: 5'-TGCTGTCCCTGTATGCCTCTG-3' and R: 5'-GCTGTAG CCACGCTCGGTC-3'. Five independent experiments were performed.

Small interfering RNA transfection

For knocking down *ARID4B* mRNA expression, three different small interfering RNA (siRNA) were designed and purchased from a company (Gene Pharma). Transfection was conducted using the transfection reagent siRNA-Mate (G04002, Gene Pharma). Briefly, 8 μ l of siRNA-Mate and 5 μ l of siRNA were mixed and then incubated with 200 μ l of OPTI-MEM I medium for 15 min, then the mixture was added into the culture medium in the well. At 24-h post-transfection, cells were harvested. The best pair of siRNAs was selected for further use by transfection

experiments and Western blotting analysis. The siRNA sequences selected for *ARID4B* knockdown were as follows: F: 5'-GCGGACAACUAGUUUCUAUTT-3' and R: 5'-AUAGAAA CUAGUUGUCCGCTT-3'. Negative control siRNA (NC) sequences were as follows: F: 5'-UUCUCCGAACGUGUCACG UTT-3' and R: 5'-ACGUGACACGUUCGGAGAATT-3'.

Transfection of *ARID4B* gene activation vectors

ARID4B has a high molecular weight (1314 aa), and it is difficult to overexpress *ARID4B* by transfection of a recombinant plasmid. The CRISPR/dCas9 technology (cotransfection into cells of SP-dcas9-VPR plasmid and gRNA targeting *ARID4B* promoter) was exploited to activate *ARID4B* gene transcription. VPR (VP64-p65-Rta) at the C-terminus of dCas9 contains three transcription factor binding domains. The co-transfection of SP-dcas9-VPR into cells with the recombinant pSPgRNA vector is able to strongly activate target gene transcription⁽⁴¹⁾. Briefly, the promoter sequence of *ARID4B* was predicted on www.Genomatrix.de, based on mouse *ARID4B* sequence (Gene ID: 94 246). Four single-guided RNAs (sgRNAs) targeting different sites of *ARID4B* promoter were designed through the bioinformatics website <http://chopchop.cbu.uib.no/>. The sgRNA sequences designed were as follows: pSPgRNA-2970: 5'-GCCTGCGTTCGACGAGAGAGGGG-3', pSPgRNA-3468: 5'-TCCCTCTCTCGTTCGAACGCAGG-3', pSPgRNA-3469: 5'-CA TAGCTGTAATAAGCTCGCAGG-3' and pSPgRNA-3470: 5'-TGC CTGCGTTCGACGAGAGAGGG-3'. These oligonucleotides were synthesised, annealed and linked to the Bbs I site under hU6 promoter of pSPgRNA expression vector (# 47 108, Addgene). The ligation product was transformed into *Escherichia coli* DH5 α (9057, TaKaRa), and the positive transformation clones were selected and sequenced. For transfection, 1.5 μ g of SP-dcas9-VPR plasmid (#63798, Addgene) and 1.5 μ g of recombinant pSPgRNA plasmid were mixed in 200 μ l of OPTI-MEM I medium, rest for 5 min; 6 μ l of GP-transfect-Mate (G04008, Gene Pharma) was added to 200 μ l of OPTI-MEM I medium, rest for 5 min. Then the two solutions were mixed and rest for 15 min before transfection. At 24 h after transfection, cells were harvested.

Genomic DNA extraction

Total genomic DNA from C2C12 cells was extracted using the Genomic DNA Mini Preparation Kit with Spin Column (D0033, Beyotime), following the manufacturer's instructions. The purity of DNA was assessed by agarose gel electrophoresis and the ratio of UV absorptions at 260 nm *v.* 280 nm.

ChIP-PCR and ChIP-qPCR

Chromatin immunoprecipitation (ChIP) assay was performed by using a ChIP Assay Kit (P2078, Beyotime), according to the manufacturer's instructions and our previous report⁽¹⁵⁾. Briefly, cells at a concentration of 3×10^6 /ml were harvested, and chromatin was cross-linked with 1% formaldehyde at 37°C for 10 min. Then the liquid was neutralised with glycine for 5 min at room temperature, next washed twice with pre-frozen PBS containing protease inhibitors. Cells were then scraped and

collected and suspended in SDS cracking buffer. Next, cells were lysed and sonicated for 10 s at 10 s intervals for fifteen times in ice water using an ultrasonic homogeniser (JY920IIN). Cell lysates were pelleted by centrifugation and resuspended in ChIP dilution buffer and incubated overnight at 4°C with anti-ARID4B (24 499–1-AP, Proteintech), anti-H3K27ac (39 034, Active Motif), anti-H3K27me3 (39 055, Active Motif) or anti-H3 (17 168–1-AP, Proteintech) antibody. Next day, 70 µl of Protein A + G Agarose/Salmon Sperm DNA was added and the solution was further incubated for 1 h. Next, the agarose was washed four times in salt solution, proteins were digested with proteinase K at 65°C for 4 h and the coprecipitated DNAs were purified. Normal Rabbit IgG (A7016, Beyotime) was used as a negative control, and RNA polymerase II (bs-6972R, Bioss) was used as a positive control. To select the possible binding sites of ARID4B in the *mTOR* promoter, twenty-four pairs of primers were designed for ChIP-PCR to amplify different regions (–1 to –5000 bp) of the *mTOR* promoter. The primer sequences were provided in online Supplemental Table S1. The efficiencies of these primers were determined by their abilities to amplify genomic DNA (see online supplementary material, Supplemental Fig. S1A). ChIP-PCR products were detected by agarose gel electrophoresis, and the positive amplification products were confirmed by sequencing and the corresponding pair of primers was used for ChIP-qPCR analysis. For ChIP-qPCR, three independent experiments were performed.

Statistical analysis

All data were presented as means and standard error for three to five independent experiments. Data statistical analysis was quantified using IBM SPSS statistical 21 software (IBM). Analysis of variance or Student's *t* test was used to determine the difference between the means. Significance was set at $P < 0.05$ or $P < 0.01$.

Results

Tau promotes protein synthesis and proliferation of C2C12 myoblast cells in a dose-dependent manner

C2C12 myoblast cells were treated with different concentrations of Tau (0, 60, 120, 180 and 240 µM) for 24 h. As the concentration of Tau increased, the protein synthesis rate gradually increased, reached a peak at 120 µM and then gradually decreased (Fig. 1(a) and (b)). The total protein content (Fig. 1(c)), cell number (Fig. 1(d) and (e)), mTOR phosphorylation (Fig. 1(f) and (g)) and S6K1 phosphorylation (Fig. 1(f) and (h)) also had the same trend. These data demonstrate that Tau can dose-dependently regulate protein synthesis and proliferation of C2C12 cells.

Tau promotes ARID4B expression in a PI3K-dependent manner

Western blotting and qRT-PCR detected that Tau treatment significantly increased the protein (Fig. 2(a) and (b)) and mRNA level (Fig. 2(c)) of ARID4B, with both reaching peak levels at 120-µM Tau treatment. PI3K inhibition by LY 294002 completely blocked Tau-stimulated AKT phosphorylation

(Fig. 2(d) and (e)), and ARID4B protein (Fig. 2(d) and (f)) and mRNA (Fig. 2(g)) expression. These data suggest that Tau increases ARID4B expression via activation of PI3K.

ARID4B is a key mediator of Tau-stimulated protein synthesis and cell proliferation

ARID4B knockdown almost totally blocked the stimulation of Tau on protein synthesis rate (Fig. 3(a) and (b)), total protein content (Fig. 3(c)) and cell number (Fig. 3(d)). To select an effective ARID4B gene activation vector (recombinant pSPgRNA), cells were co-transfected with the SP-dcas9-VPR vector and pSPgRNA-2970, pSPgRNA-3468, pSPgRNA-3469 or pSPgRNA-3470 vector. Western blotting detected that both pSPgRNA-3469 and pSPgRNA-3470 significantly stimulated ARID4B expression (Fig. 4(a) and (b)). The protein synthesis rate (Fig. 4(c) and (d)), total protein content (Fig. 4(e)) and cell number (Fig. 4(f)) were all significantly increased in cells of ARID4B gene activation. Taken together, these above data demonstrate that ARID4B is a key mediator for the stimulation of Tau on protein synthesis and cell proliferation.

ARID4B mediates the stimulation of Tau on the mTOR signalling

ARID4B knockdown (Fig. 5(a) and (b)) almost totally abrogated the stimulation of Tau on the phosphorylation of mTOR (Fig. 5(a) and (c)) and S6K1 (Fig. 5(a) and (d)), whereas ARID4B gene activation (Fig. 5(e) and (f)) significantly increased mTOR (Fig. 5(e) and (g)) and S6K1 (Fig. 5(e) and (h)) phosphorylation. qRT-PCR analysis further detected that ARID4B knockdown almost totally blocked the stimulation of Tau on the mRNA expression of *mTOR* (Fig. 5(i)), whereas ARID4B gene activation significantly promoted this expression (Fig. 5(j)). These data suggest that ARID4B mediates the stimulation of Tau on mRNA expression and subsequent protein phosphorylation of mTOR.

Tau stimulates the binding of ARID4B to the mTOR promoter

ChIP-PCR analysis was performed to find the possible binding site of ARID4B in the *mTOR* promoter (–1 ~ –5000 bp). Agarose gel electrophoresis detected that only one product (–4368 to –4591 bp) was obtained from ChIP-PCR with the twenty-four pairs of specific primers (online Supplemental Fig. S1(B), Fig. 6(a)). ChIP-qPCR analysis further detected that Tau treatment significantly promoted the binding of ARID4B to this region (Fig. 6(b)), suggesting that ARID4B mediates Tau signalling to gene transcription of *mTOR* via binding to its promoter.

ARID4B mediates the stimulation of Tau on the binding of H3K27ac to the mTOR promoter

We then determined whether ARID4B affects the protein levels and promoter binding ability of the two histone modifications H3K27ac and H3K27me3. Western blotting detected that ARID4B knockdown (Fig. 7(a)) or gene activation (Fig. 7(b)) did not affect the protein levels of H3K27ac and H3K27me3 in cells. Actinomycin D (Act D, a RNAPII transcription inhibitor)



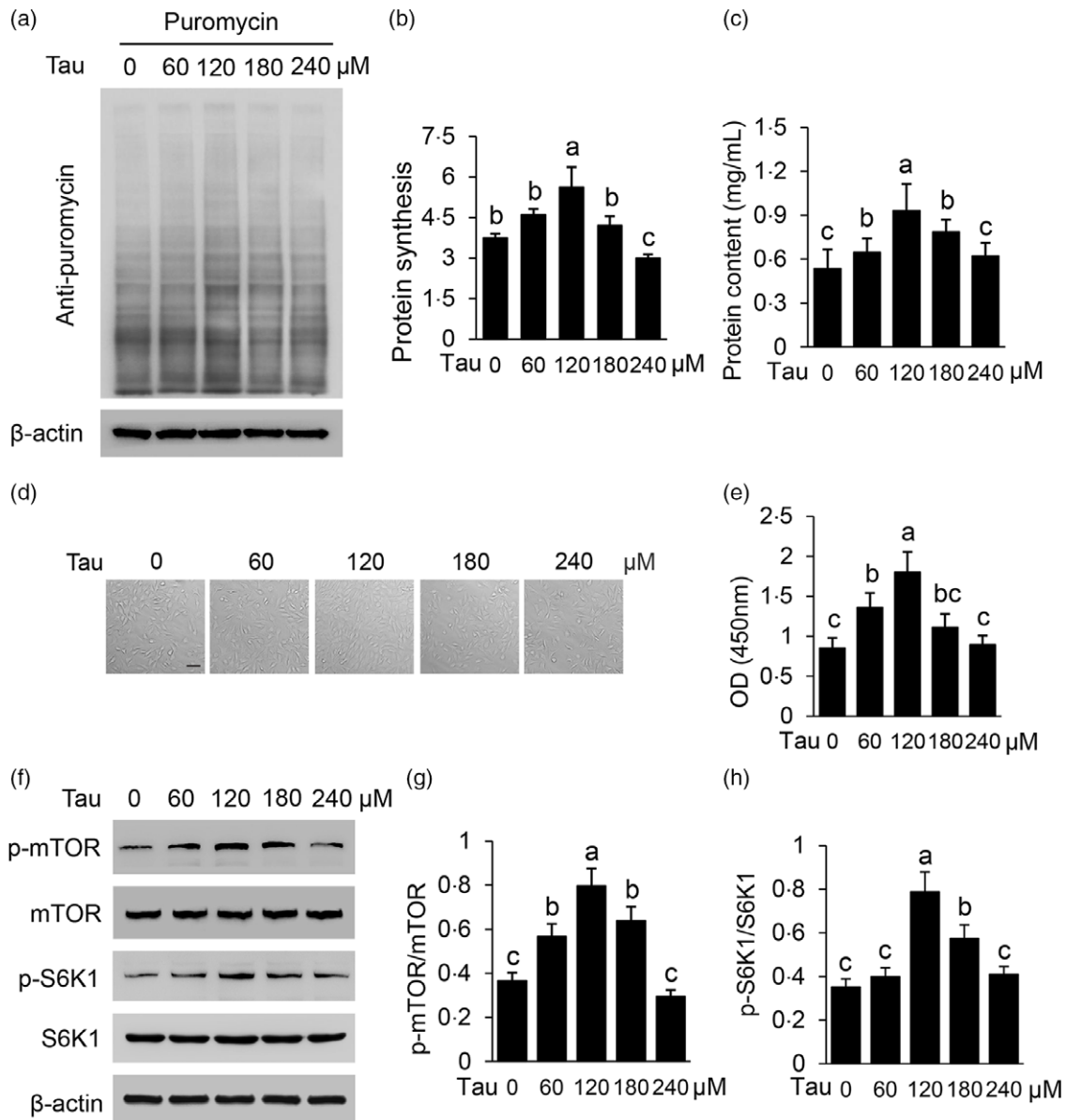


Fig. 1. Effects of Tau on protein synthesis and cell proliferation. (a) C2C12 cells were treated with different concentrations of Tau (0, 60, 120, 180 and 240 μM) for 24 h. The protein synthesis rate was detected using the SUNSET method. (b) Total protein/ β -actin relative levels of Western blots in (a) were quantified by grey scale scanning. (c) The total protein content in C2C12 cells was detected using a BCA protein concentration determination kit. (d) Cell morphological images were observed by an inverted microscope. Scale bar represents 55 μm. (e) Cell number was detected using a CCK-8 assay kit. (f) Indicated protein levels in C2C12 cells were analysed by Western blotting analysis. (g) and (h) The ratio of p-mTOR/mTOR (g) and p-S6K1/S6K1 (h) of Western blots in (f) were quantified. Data are the mean \pm SE of independent experiments (n 3 in (a), (f), n 5 in (c), (e)). ^{a,b,c} Mean values with unlike letters were significantly different ($P < 0.05$). Tau, Taurine; SUNSET, surface sensing of translation; mTOR, mechanistic target of rapamycin protein; S6K1, S6 kinase 1.

did not affect the protein levels of these two histone modifications, suggesting that their levels are stable in the nucleus and not closely related to their gene expression (Fig. 7(a) and (b)). Interestingly, ChIP-PCR analysis detected the same binding site (-4368 to -4591 bp) of H3K27ac (Online Supplemental Fig. S2) and H3K27me3 (Fig. S3) in the *mTOR* promoter (-1 ~ -5000 bp). ChIP-qPCR further detected that ARID4B knockdown hindered the binding of H3K27ac (Fig. 7(c)) but did not affect the binding of H3K27me3 (Fig. 7(d)) to the *mTOR* promoter. ARID4B gene activation promoted H3K27ac (Fig. 7(e)) but did not affect H3K27me3 (Fig. 7(f)) binding to the *mTOR* promoter.

Furthermore, ARID4B knockdown almost totally blocked the stimulation of Tau on H3K27ac deposition on the *mTOR* promoter (Fig. 7(g)). These data demonstrate that ARID4B mediates the stimulation of Tau on the binding of H3K27ac to the *mTOR* promoter.

Discussion

It is largely unknown whether Tau can regulate the mTOR pathway and anabolism in muscle cells through an epigenetic

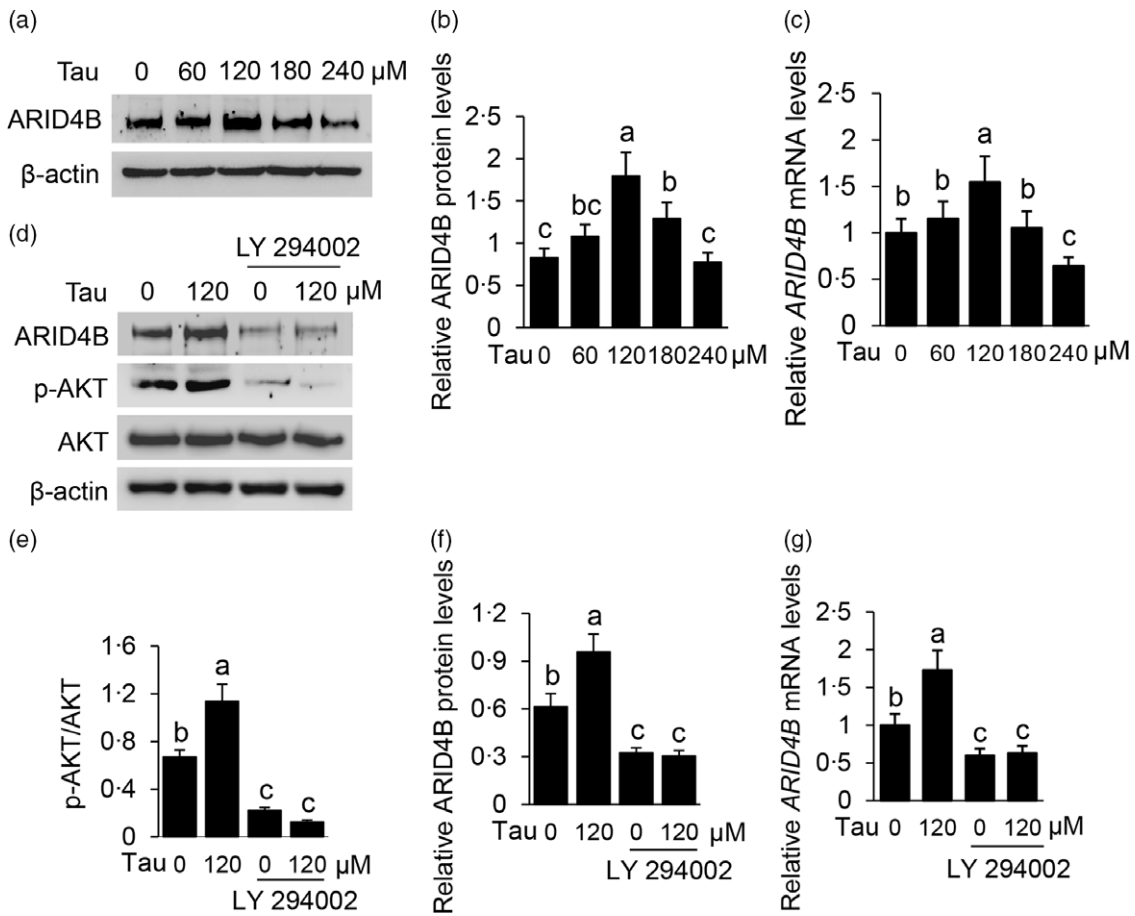


Fig. 2. Effects of Tau and PI3K on ARID4B expression. (a) Cells were treated as in Fig. 1. ARID4B protein levels were analysed by Western blotting analysis. (b) ARID4B/ β -actin relative levels of Western blots in (a) were quantified by grey scale scanning. (c) qRT-PCR analysis of *ARID4B* mRNA level in cells treated as in (a). (d) C2C12 cells were treated with Tau (120 μ M) and LY 294002 (15 μ M) for 24 h. Indicated protein levels were analysed by Western blotting analysis. (e) The ratio of p-AKT:AKT of Western blots in (d) were quantified. (f) ARID4B/ β -actin relative levels of Western blots in (d) were quantified. (g) qRT-PCR analysis of *ARID4B* mRNA level in cells treated as in (d). Data are the mean \pm SE of independent experiments (n 3 in (a), (d), n 5 in (c), (g)). ^{a,b,c} Mean values with unlike letters were significantly different ($P < 0.05$). Tau, Taurine; PI3K, phosphoinositide 3-kinase; ARID4B, AT-rich interaction domain 4B.

regulatory mechanism. In this study, we demonstrate that Tau promotes protein synthesis and proliferation of C2C12 cells in a dose-dependent manner. Tau stimulates ARID4B expression through the PI3K signalling, and ARID4B mediates Tau signalling to mRNA expression and subsequent protein phosphorylation of mTOR. Tau stimulates ARID4B binding to the promoter of *mTOR*, and ARID4B mediates the stimulation of Tau on H3K27ac deposition on the *mTOR* promoter.

We observed that Tau promoted protein synthesis, cell proliferation, mRNA expression and protein phosphorylation of mTOR, S6K1 phosphorylation and ARID4B expression in a dose-dependent manner when Tau concentration was lower than 120 μ M. High concentrations of Tau (higher than 120 μ M) had opposite effects. Recent reports show that the plasma concentrations of Tau in starter pigs are ranged from 40 to 50 μ M⁽⁴²⁾, while those in Huanjiang minipigs during gestation period are ranged from 110 to 135 μ M⁽⁴³⁾. The plasma Tau concentrations of dogs fed a nutrient-fortified endurance diet

containing 0.34% Tau over several months were ranged from 145 to 180 μ M, which were markedly higher than those of the control fed a diet containing 0.07% Tau (ranged from 60 to 90 μ M)⁽⁴⁴⁾. From these reports, we consider that the best concentration of Tau (120 μ M) to promote protein synthesis and proliferation of C2C12 cells cultured *in vitro* is basically in agreement with the plasma Tau concentrations in animals. Diets containing no more than 0.5% and 0.4–0.8% (w/w) Tau can increase the growth performance of broiler chickens and crabs, respectively^(22,24). From these above reports, we speculate that diet supplemented with 0.3–0.8% Tau might be beneficial to the growth performance of animals.

High doses of Tau in the diet can be toxic for animals. Diets containing 0.3% Tau for 28 d could promote growth performance and liver and intestinal health of weaned piglets, while 1.5% Tau had adverse effects⁽⁴⁵⁾. Excessive Tau inhibits the activities of catalase and superoxide dismutase in human nerve cells, leading to cell apoptosis⁽⁴⁶⁾. Isethionic acid and

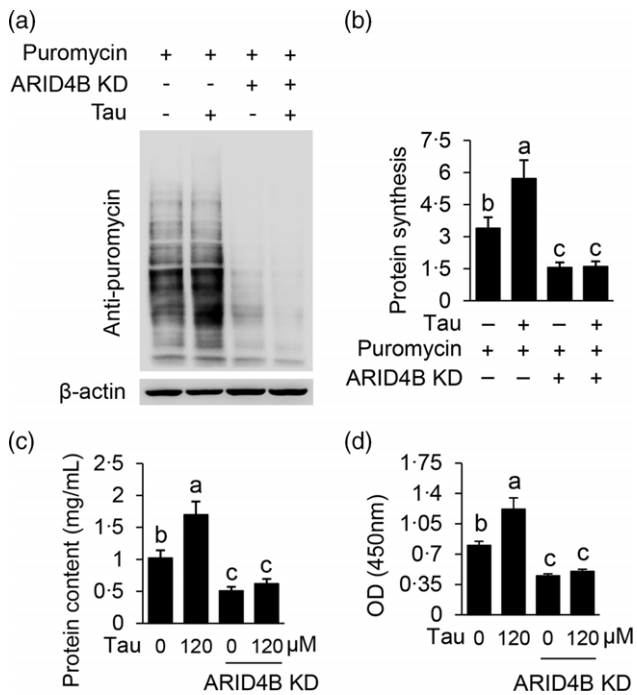


Fig. 3. Effects of ARID4B knockdown on Tau-stimulated protein synthesis and cell proliferation. (a) C2C12 cells were transfected with an ARID4B siRNA and treated with Tau (120 μ M) for 24 h. Protein synthesis rate was analysed by Western blotting analysis using an antibody against puromycin. (b) Total protein/ β -actin relative levels of Western blots in (a) were quantified by grey scale scanning. (c) The total protein content in cells treated as in (a) was detected using a BCA protein concentration determination kit. (d) Number of cells treated as in (a) was detected using a CCK-8 assay kit. Data are the mean \pm SE of independent experiments (n 3 in (a), n 5 in (c), (d)). ^{a,b,c} Mean values with unlike letters were significantly different ($P < 0.05$). ARID4B, AT-rich interaction domain 4B; Tau, Taurine.

sulfoacetaldehyde are formed by the oxidation of excessive Tau, indicating that excessive Tau may be cytotoxic⁽⁴⁷⁾. A previous report pointed out a promising approach for the use of a lower dose of Tau combined with branched-chain amino acids for muscle cell growth⁽⁴⁸⁾. From our experimental data and previous reports, we conclude that Tau promotes protein synthesis and proliferation of C2C12 cells in a dose-dependent manner, and excessive Tau has toxic effects. Our findings provide reference data for the application of Tau in skeletal muscle growth and protein production in animal feeding.

Our data showed that PI3K was required for Tau to stimulate ARID4B expression. Previous reports have validated that Tau can promote cell proliferation and inhibit cell apoptosis in a PI3K-dependent manner^(15,49,50), in agreement with our data. It is still largely unclear the molecular mechanism via which Tau can activate PI3K. Previous reports have shown that Tau can promote PI3K activation through the G protein-coupled receptor 87 (GPR87)⁽¹⁵⁾ or TauT including TauT/SLC6A6 and PAT1/SLC36A1⁽⁵¹⁾. Future studies should explore the roles of GPCR and TauT in Tau signalling to PI3K activation. The PI3K signalling network can regulate diverse downstream signalling pathways to control transcription factors and affect gene expression⁽⁵²⁾. The detailed molecular mechanism through

which Tau stimulated mRNA expression of ARID4B is still unknown and awaits further study.

Our gene function study data showed that ARID4B mediated the stimulation of Tau on protein synthesis, cell proliferation, mRNA expression and protein phosphorylation of mTOR, and mTOR target S6K1 phosphorylation. Previous reports have confirmed that Tau can directly stimulate the PI3K-AKT-mTOR signalling, but it is rarely reported that Tau can activate the mTOR pathway through stimulating its mRNA expression. Our data demonstrate that ARID4B mediates Tau signalling to mRNA expression and subsequent protein phosphorylation of mTOR. In agreement with our previous observation^(15,53), as is expected, the phosphorylated form of mTOR was changed according to its mRNA level, while the unphosphorylated form of mTOR remained stable. We speculate that the stable mTOR protein levels and variable mTOR mRNA and p-mTOR levels are a mechanism for cells to respond quickly to intracellular and extracellular stimuli. Previous reports have pointed that ARID4B has a variety of regulatory roles in cell proliferation and differentiation, and the normal development and physiological process⁽³⁵⁻³⁹⁾, in agreement with our results. Our findings reveal another layer of Tau regulation of the mTOR-S6K1 signalling pathway, emphasising the importance of gene expression regulation in Tau-stimulated mTOR activation.

ARID4B has a DNA binding domain of spiral-rotation-helical structure comprised approximately 100 amino acid residues, and the disordered C-terminus provides an additional DNA binding site⁽⁵⁴⁾. The molecular mechanism through which ARID4B regulates gene expression is just emerging, and the binding site of ARID4B on the *mTOR* promoter has not been identified. In this study, CHIP-PCR detected that ARID4B bound to the -4368 to -4591 bp site of the *mTOR* promoter, and CHIP-qPCR further detected that Tau stimulated ARID4B binding to this site. Our data suggest that ARID4B mediates Tau stimulation on *mTOR* mRNA expression through its binding to the *mTOR* promoter and thereby affecting its gene transcription.

Histone modification plays an important role in regulating gene expression during mammalian growth and development. Numerous reports have established that the two histone modifications H3K27ac and H3K27me3 can bind to gene promoters (enhancers) and are well known as gene activating and gene silencing markers, respectively⁽⁵⁵⁻⁵⁷⁾. Interestingly, we found ARID4B, H3K27ac and H3K27me3 bound only to one distal site (which might be an enhancer region) in the *mTOR* promoter (-1 to -5000 bp). Furthermore, Tau stimulated the binding of ARID4B to this site, and ARID4B mediated Tau stimulation of the binding of H3K27ac but not H3K27me3 to this site. Previous reports have uncovered that ARID4B is a member of the chromatin remodelling complex SIN3A/HDAC1, which lacks methyltransferase or acetyl transferase activity and might function through inhibiting HDAC1 expression^(34,37,57). It is still unclear the detailed mechanism via which ARID4B regulates the binding of H3K27ac to its promoters, which awaits further investigations. Our experimental results demonstrate that Tau increases ARID4B binding to the *mTOR* promoter and thereby triggers the binding of H3K27ac to the same site.

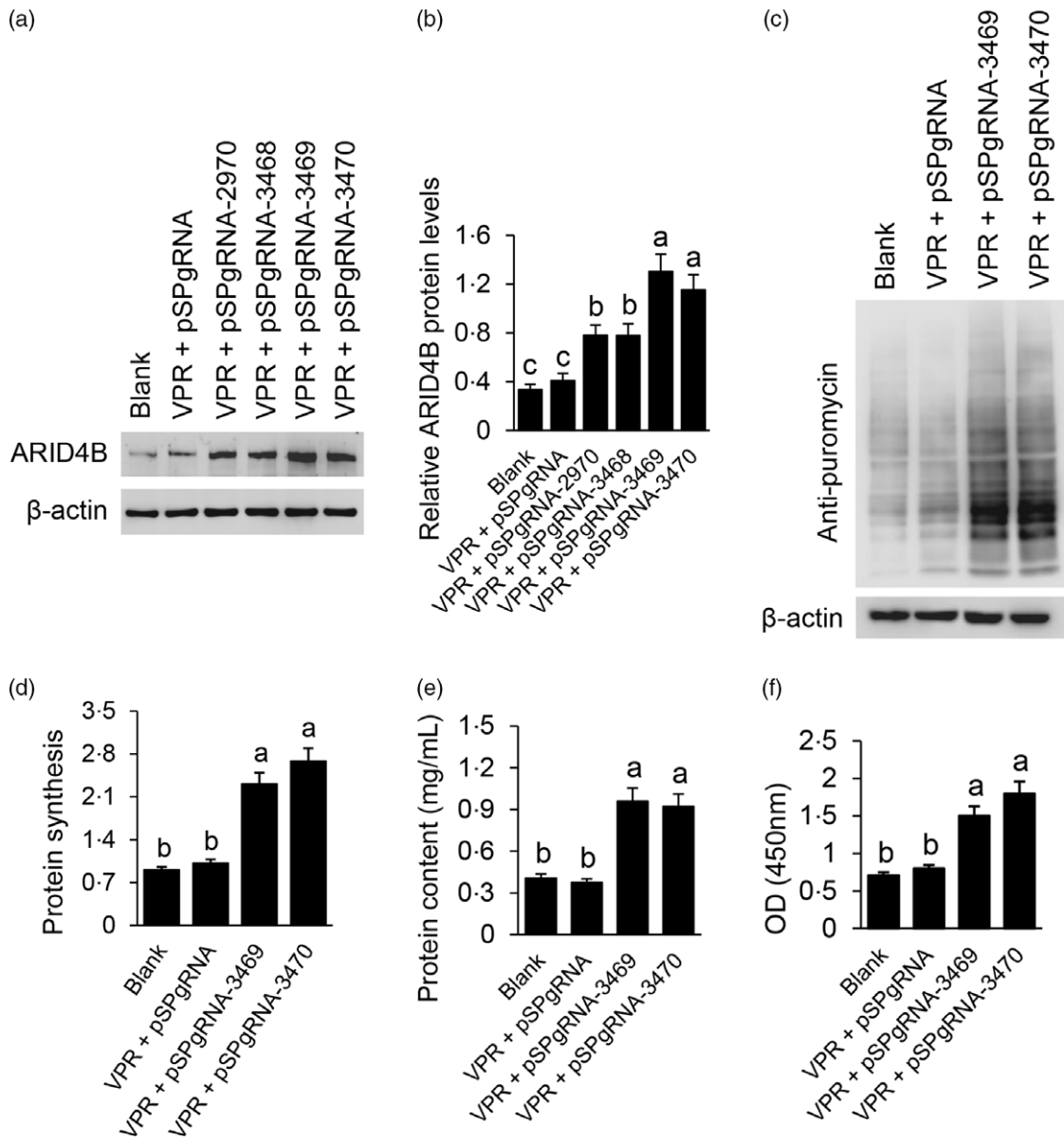


Fig. 4. Effects of ARID4B gene activation on protein synthesis and cell proliferation. (a) ARID4B protein level was detected by Western blotting in cells transfected with indicated vectors. (b) ARID4B/ β -actin relative levels of Western blots in (a) were quantified by grey scale scanning. (c) Protein synthesis rate in cells transfected with indicated vectors was analysed by Western blotting analysis. (d) Total protein/ β -actin relative levels of Western blots in (c) were quantified. (e) The total protein content in cells treated as in (c) was detected. (f) Number of cells treated as in (c) was detected. Data are the mean \pm SE of independent experiments (n 3 in (a), (c), n 5 in (E), (f)). ^{a,b,c} Mean values with unlike letters were significantly different ($P < 0.05$). ARID4B, AT-rich interaction domain 4B.

Conclusion

In summary, current work uncovers that Tau can dose-dependently promote protein synthesis and proliferation of C2C12 cells through the PI3K-ARID4B-mTOR pathway. ARID4B mediates Tau stimulation on mRNA expression of *mTOR* through regulating H3K27ac binding to the *mTOR* promoter. Our findings provide a deep understanding of how Tau epigenetically regulates anabolism in muscle cells.

Acknowledgements

This work was supported by grants from National Natural Science Foundation of China (No. 31671473).

Q. H. and L. W. designed the research and performed the experiments; M. Z. and Z. W. analysed the results; M. L. provided critical reagents; X. G. and Q. H. wrote and reviewed the manuscript.

The authors declare no conflict of interest.

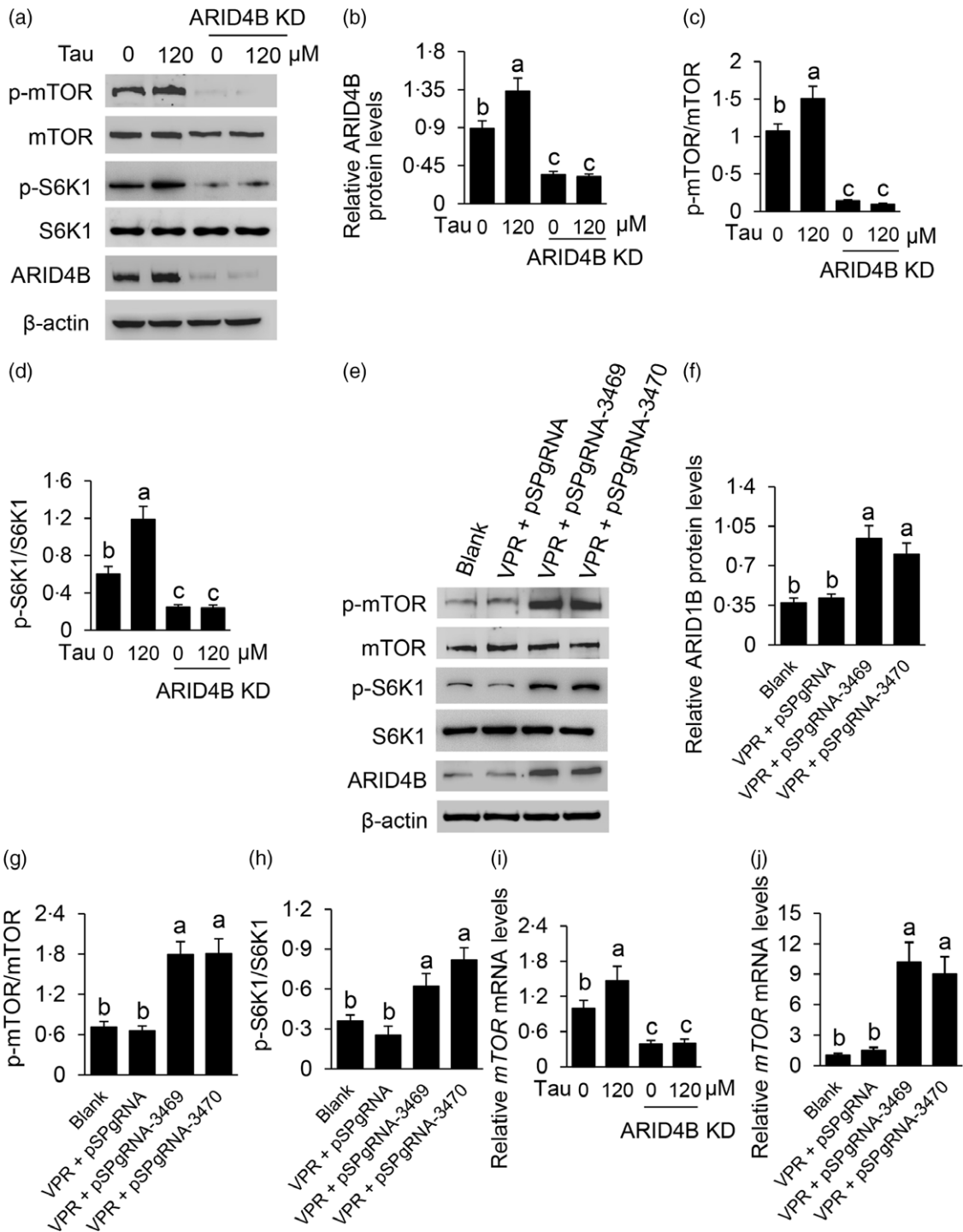


Fig. 5. Effects of ARID4B on Tau-stimulated mRNA expression and phosphorylation of mTOR. (a) Cells were treated with Tau and transfected with an ARID4B siRNA for 24 h. Indicated protein levels were analysed by Western blotting analysis. (b) ARID4B/ β -actin relative levels of Western blots in (a) were quantified by grey scale scanning. (c) and (d) The ratio of p-mTOR/mTOR (c) and p-S6K1/S6K1 (d) of Western blots in (a) were quantified. (e) Cells were transfected with the VPR together with pSPgRNA3469 or pSPgRNA3470 plasmid. Indicated protein levels were analysed by Western blotting analysis. (f) ARID4B/ β -actin relative levels of Western blots in (e) were quantified by grey scale scanning. (g) and (h) The ratio of p-mTOR/mTOR (g) and p-S6K1/S6K1 (h) of Western blots in (e) were quantified. (i) and (j) Cells were treated as in Fig. 3(a) (i) and Fig. 4(c) (j). The mRNA levels of *mTOR* were detected by qRT-PCR. Data are the mean \pm SE of independent experiments (n 3 in (a), (e), n 5 in (i), (j)). ^{a,b,c} Mean values with unlike letters were significantly different ($P < 0.05$). ARID4B, AT-rich interaction domain 4B; Tau, Taurine; mTOR, mechanistic target of rapamycin protein; S6K1, S6 kinase 1;

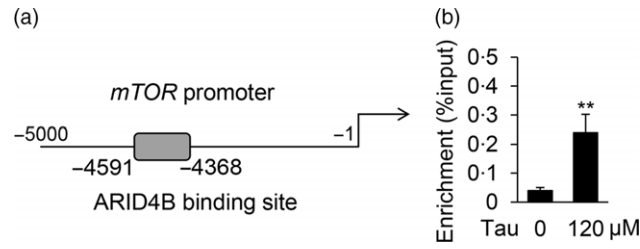


Fig. 6. The effect of Tau on the binding of ARID4B to the mTOR promoter. (a) ChIP-PCR analysis of the binding site of ARID4B in the *mTOR* gene promoter. Twenty-four pairs of primers were designed for ChIP-PCR to amplify different regions of the *mTOR* gene promoter (–1 to –5000 bp). Only one sequence (–4368 to –4591 bp) was amplified in the *mTOR* promoter, and this primer was used next for ChIP-qPCR. Diagram depicts the binding region of ARID4B in the promoter of *mTOR*. (b) ChIP-qPCR analysis to determine the effect of Tau on the binding of ARID4B to the promoter of *mTOR*. Data are the mean \pm SE of three independent experiments. ^{***}, $P < 0.01$. Tau, Taurine; ARID4B, AT-rich interaction domain 4B; mTOR, mechanistic target of rapamycin protein; ChIP, chromatin immunoprecipitation.

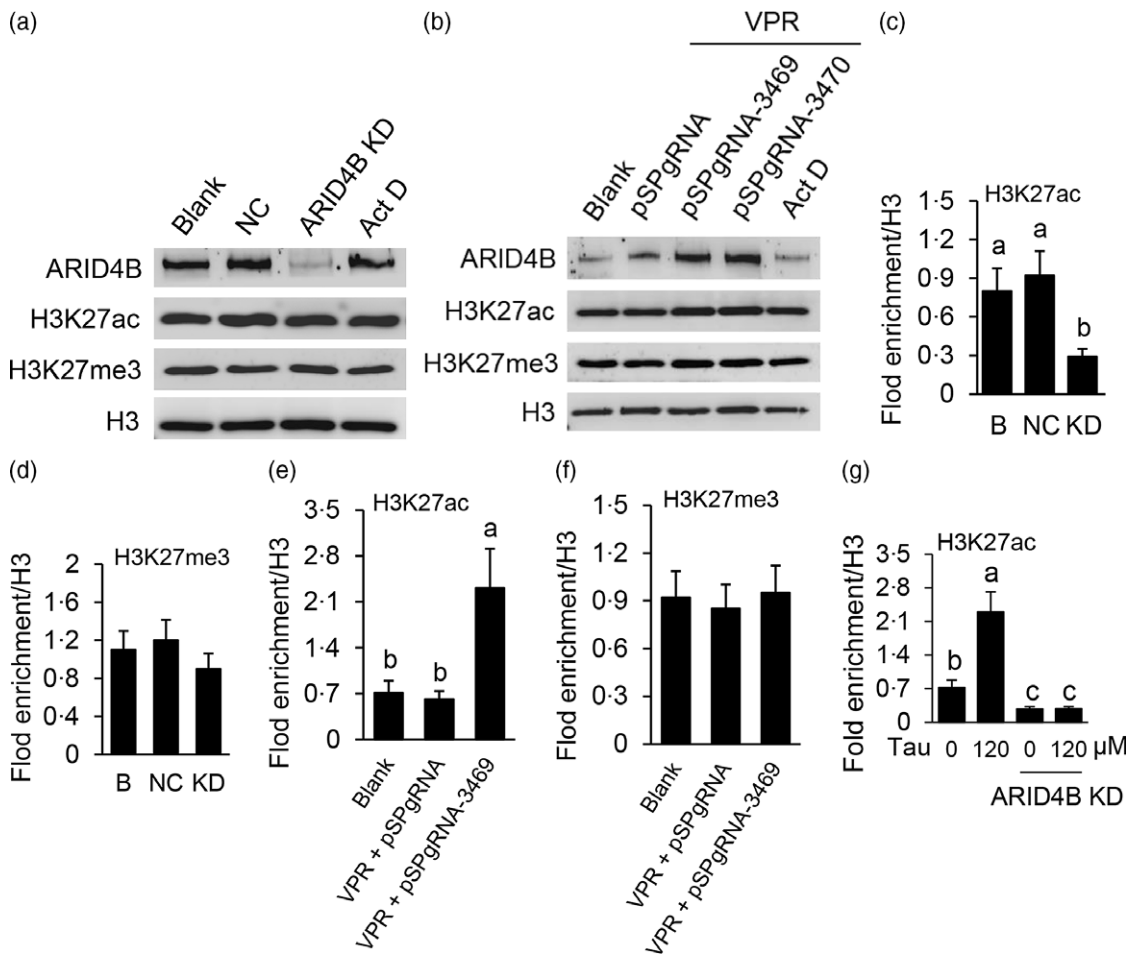


Fig. 7. Effects of ARID4B on the stimulation of Tau on H3K27ac binding to the mTOR promoter. (a) and (b) Western blotting analysis were performed to determine indicated protein levels in cells transfected with an ARID4B siRNA (a) or ARID4B gene activation vectors (b). Cells treated with Act D were used as an experimental control. (c) and (d) ChIP-qPCR analysis of the binding of H3K27ac (c) and H3K27me3 (d) to the *mTOR* promoter in cells transfected with an ARID4B siRNA. (e) and (f) ChIP-qPCR analysis of the binding of H3K27ac (e) and H3K27me3 (f) to the *mTOR* promoter in cells transfected with ARID4B gene activation vectors. (g) ChIP-qPCR analysis of the binding of H3K27ac to the *mTOR* promoter in cells treated with Tau and transfected with an ARID4B siRNA. Data are the mean \pm SE of three independent experiments. ^{a,b,c} Mean values with unlike letters were significantly different ($P < 0.05$). ARID4B, AT-rich interaction domain 4B; Tau, Taurine; mTOR, mechanistic target of rapamycin protein; siRNA, small interfering RNA; Act D, Actinomycin D; ChIP, chromatin immunoprecipitation.

Supplementary material

For supplementary material/s referred to in this article, please visit <https://doi.org/10.1017/S0007114521004918>

References

- Shamim B, Hawley JA & Camera DM (2018) Protein availability and satellite cell dynamics in skeletal muscle. *Sports Med* **48**, 1329–1343.
- Saxton RA & Sabatini DM (2017) mTOR signaling in growth, metabolism, and disease. *Cell* **168**, 960–976.
- Liu GY & Sabatini DM (2020) mTOR at the nexus of nutrition, growth, ageing and disease. *Nat Rev Mol Cell Biol* **21**, 183–203.
- Wolfson RL & Sabatini DM (2017) The dawn of the age of amino acid sensors for the mTORC1 pathway. *Cell Metab* **26**, 301–309.
- Magnuson B, Ekim B & Fingar DC (2012) Regulation and function of ribosomal protein S6 kinase (S6K) within mTOR signalling networks. *Biochem J* **441**, 1–21.
- Hua H, Kong Q, Zhang H, et al. (2019) Targeting mTOR for cancer therapy. *J Hematol Oncol* **12**, 71.
- Schiaffino S, Dyar KA, Ciciliot S, et al. (2013) Mechanisms regulating skeletal muscle growth and atrophy. *FEBS J* **280**, 4294–4314.
- Schiaffino S, Reggiani C, Akimoto T, et al. (2021) Molecular mechanisms of skeletal muscle hypertrophy. *J Neuromuscul Dis* **8**, 169–183.
- Spriet LL & Whitfield J (2015) Taurine and skeletal muscle function. *Curr Opin Clin Nutr Metab Care* **18**, 96–101.
- Thirupathi A, Pinho RA, Baker JS, et al. (2020) Taurine reverses oxidative damages and restores the muscle function in overuse of exercised muscle. *Front Physiol* **11**, 582449.
- EI Idrissi A (2019) Taurine regulation of neuroendocrine function. *Adv Exp Med Biol* **1155**, 977–985.
- Jakaria M, Azam S, Haque ME, et al. (2019) Taurine and its analogs in neurological disorders: focus on therapeutic potential and molecular mechanisms. *Redox Biol* **24**, 101223.
- You G, Long X, Song F, et al. (2020) Metformin activates the AMPK-mTOR pathway by modulating lncRNA *TUG1* to induce autophagy and inhibit atherosclerosis. *Drug Devel Ther* **14**, 457–468.
- Anderson CM, Howard A, Walters JR, et al. (2009) Taurine uptake across the human intestinal brush-border membrane is via two transporters: H⁺-coupled PAT1 (SLC36A1) and Na⁺- and Cl⁻-dependent TauT (SLC6A6). *J Physiol* **587**, 731–744.
- Yu M, Wang Y, Wang Z, et al. (2019) Taurine promotes milk synthesis via the GPR87-PI3K-SETD1A signaling in BMECs. *J Agric Food Chem* **67**, 1927–1936.
- Solon CS, Franci D, Ignacio-Souza LM, et al. (2012) Taurine enhances the anorexigenic effects of insulin in the hypothalamus of rats. *Amino Acids* **42**, 2403–2410.
- Wang Z, Lan R, Xu Y, et al. (2021) Taurine alleviates *Streptococcus uberis*-induced inflammation by activating autophagy in mammary epithelial cells. *Front Immunol* **12**, 631113.
- Zhai N, Wang H, Chen Y, et al. (2018) Taurine attenuates OTA-promoted PCV2 replication through blocking ROS-dependent autophagy via inhibiting AMPK/mTOR signaling pathway. *Chem Biol Interact* **296**, 220–228.
- Sun Y, Dai S, Tao J, et al. (2020) Taurine suppresses ROS-dependent autophagy via activating Akt/mTOR signaling pathway in calcium oxalate crystals-induced renal tubular epithelial cell injury. *Aging* **12**, 17353–17366.
- Yu M, Wang Y, Li P, et al. (2020) Taurine attenuates gossypol-induced apoptosis of C2C12 mouse myoblasts via the GPR87-AMPK/AKT signaling. *Amino Acids* **52**, 1285–1298.
- Wen C, Li F, Zhang L, et al. (2019) Taurine is involved in energy metabolism in muscles, adipose tissue, and the liver. *Mol Nutr Food Res* **63**, e1800536.
- Han HL, Zhang JF, Yan EF, et al. (2020) Effects of taurine on growth performance, antioxidant capacity, and lipid metabolism in broiler chickens. *Poult Sci* **99**, 5707–5717.
- Zafalon RVA, Risolia LW, Vendramini THA, et al. (2020) Nutritional inadequacies in commercial vegan foods for dogs and cats. *PLOS ONE* **15**, e0227046.
- Dong J, Cheng R, Yang Y, et al. (2018) Effects of dietary taurine on growth, non-specific immunity, anti-oxidative properties and gut immunity in the Chinese mitten crab *Eriocheir sinensis*. *Fish Shellfish Immunol* **82**, 212–219.
- Zhou Z, Ferdous F, Montagner P, et al. (2018) Methionine and choline supply during the peripartur period alter polymorphonuclear leukocyte immune response and immunometabolic gene expression in Holstein cows. *J Dairy Sci* **101**, 10374–10382.
- Seidel U, Huebbe P & Rimbach G (2019) Taurine: a regulator of cellular redox homeostasis and skeletal muscle function. *Mol Nutr Food Res* **63**, e1800569.
- Miyazaki T, Honda A, Ikegami T, et al. (2013) The role of taurine on skeletal muscle cell differentiation. *Adv Exp Med Biol* **776**, 321–328.
- Wen C, Li F, Guo Q, et al. (2020) Protective effects of taurine against muscle damage induced by diquat in 35 d weaned piglets. *J Anim Sci Biotechnol* **11**, 56.
- Zhou L, Lu R, Huang C, et al. (2021) Taurine protects C2C12 myoblasts from impaired cell proliferation and myotube differentiation under cisplatin-induced ROS exposure. *Front Mol Biosci* **8**, 685362.
- Barbiera A, Sorrentino S, Lepore E, et al. (2020) Taurine attenuates catabolic processes related to the onset of sarcopenia. *Int J Mol Sci* **21**, 8865.
- Wilsker D, Probst L, Wain HM, et al. (2005) Nomenclature of the ARID family of DNA-binding proteins. *Genomics* **86**, 242–251.
- Zhang J, Hou S, You Z, et al. (2021) Expression and prognostic values of ARID family members in breast cancer. *Aging* **13**, 5621–5637.
- Wu RC, Young IC, Chen YF, et al. (2019) Identification of the PTEN-ARID4B-PI3K pathway reveals the dependency on ARID4B by PTEN-deficient prostate cancer. *Nat Commun* **10**, 4332.
- Fleischer TC, Yun UJ & Ayer DE (2003) Identification and characterization of three new components of the mSin3A corepressor complex. *Mol Cell Biol* **23**, 3456–3467.
- Keskin EG, Huang J & Terzi Çizmeçioğlu N (2021) Arid4b physically interacts with Tfp2c in mouse embryonic stem cells. *Turk J Biol* **45**, 162–170.
- Terzi Cizmeçioğlu N, Huang J, Keskin EG, et al. (2020) ARID4B is critical for mouse embryonic stem cell differentiation towards mesoderm and endoderm, linking epigenetics to pluripotency exit. *J Biol Chem* **295**, 17738–17751.
- Luo SM, Tsai WC, Tsai CK, et al. (2021) ARID4B knockdown suppresses PI3K/AKT signaling and induces apoptosis in human glioma cells. *Onco Targets Ther* **14**, 1843–1855.
- Wang Y, Lou N, Zuo M, et al. (2021) STAT3-induced ZBED3-AS1 promotes the malignant phenotypes of melanoma cells by activating PI3K/AKT signaling pathway. *RNA Biol* (In the Press).
- Goodman CA, Mabrey DM, Frey JW, et al. (2011) Novel insights into the regulation of skeletal muscle protein synthesis as revealed by a new nonradioactive *in vivo* technique. *FASEB J* **25**, 1028–1039.

40. Schmidt EK, Clavarino G, Ceppi M, *et al.* (2009) SUnSET, a nonradioactive method to monitor protein synthesis. *Nat Methods* **6**, 275–277.
41. Chavez A, Scheiman J, Vora S, *et al.* (2015) Highly efficient Cas9-mediated transcriptional programming. *Nat Methods* **12**, 326–328.
42. Rakhshandeh A, de Lange CFM, Htoo JK, *et al.* (2020) Immune system stimulation increases the irreversible loss of cysteine to taurine, but not sulfate, in starter pigs. *J Anim Sci* **98**, skaa001.
43. Zhu Q, Xie P, Li H, *et al.* (2021) Dynamic changes of metabolite profiles in maternal biofluids during gestation period in Huanjiang mini-pigs. *Front Vet Sci* **8**, 636943.
44. Beloshapka AN, de Godoy MRC, Carter RA, *et al.* (2018) Longitudinal changes in blood metabolites, amino acid profile, and oxidative stress markers in American Foxhounds fed a nutrient-fortified diet. *J Anim Sci* **96**, 930–940.
45. Liu Y, Mao X, Yu B, *et al.* (2014) Excessive dietary taurine supplementation reduces growth performance, liver and intestinal health of weaned pigs. *Livest Sci* **168**, 109–119.
46. Zeidán-Chuliá F, Gelain DP, Kolling EA, *et al.* (2013) Major components of energy drinks (caffeine, taurine, and guarana) exert cytotoxic effects on human neuronal SH-SY5Y cells by decreasing reactive oxygen species production. *Oxid Med Cell Longev* **2013**, 791795.
47. Weinitschke S, von Rekowski KS, Denger K, *et al.* (2005) Sulfoacetaldehyde is excreted quantitatively by *Acinetobacter calcoaceticus* SW1 during growth with taurine as sole source of nitrogen. *Microbiology* **151**, 1285–1290.
48. Ra SG, Miyazaki T, Ishikura K, *et al.* (2013) Combined effect of branched-chain amino acids and taurine supplementation on delayed onset muscle soreness and muscle damage in high-intensity eccentric exercise. *J Int Soc Sports Nutr* **10**, 51.
49. Li K, Wang D, Zhou X, *et al.* (2019) Taurine protects against arsenic-induced apoptosis via PI3K/Akt pathway in primary cortical neurons. *Adv Exp Med Biol* **1155**, 747–754.
50. Han L, Yang J, Jing L, *et al.* (2019) Tau-TCHF inhibits splenic apoptosis via PI3K-Akt signaling pathway in chickens. *Adv Exp Med Biol* **1155**, 555–563.
51. Baliou S, Kyriakopoulos AM, Goulielmaki M, *et al.* (2020) Significance of taurine transporter (TauT) in homeostasis and its layers of regulation (review). *Mol Med Rep* **22**, 2163–2173.
52. Hoxhaj G & Manning BD (2020) The PI3K-AKT network at the interface of oncogenic signalling and cancer metabolism. *Nat Rev Cancer* **20**, 74–88.
53. Huo N, Yu M, Li X, *et al.* (2019) PURB is a positive regulator of amino acid-induced milk synthesis in bovine mammary epithelial cells. *J Cell Physiol* **234**, 6992–7003.
54. Ren J, Yao H, Hu W, *et al.* (2021) Structural basis for the DNA-binding activity of human ARID4B Tudor domain. *J Biol Chem* **296**, 100506.
55. Yao J, Chen J, Li LY, *et al.* (2020) Epigenetic plasticity of enhancers in cancer. *Transcription* **11**, 26–36.
56. Katoh N, Kuroda K, Tomikawa J, *et al.* (2018) Reciprocal changes of H3K27ac and H3K27me3 at the promoter regions of the critical genes for endometrial decidualization. *Epigenomics* **10**, 1243–1257.
57. Lai A, Kennedy BK, Barbie DA, *et al.* (2001) RBP1 recruits the mSIN3-histone deacetylase complex to the pocket of retinoblastoma tumor suppressor family proteins found in limited discrete regions of the nucleus at growth arrest. *Mol Cell Biol* **21**, 2918–2932.